Frank, U. (2007): Palaeomagnetic investigations on lake sediments from NE China: a new record of geomagnetic secular variations for the last 37 ka. - Geophysical Journal International, 169, 1, pp. 29—40.

DOI: http://doi.org/10.1111/j.1365-246X.2006.03272.x

Geophys. J. Int. (2007) **169,** 29–40 doi: 10.1111/j.1365-246X.2006.03272.x

Palaeomagnetic investigations on lake sediments from NE China: a new record of geomagnetic secular variations for the last 37 ka

Ute Frank

GeoForschungsZentrum Potsdam, Section 3.3. *Climate dynamics and sedimentation, Telegrafenberg,* D-14473 *Potsdam, Germany.*
E-mail: ufrank@gfz-potsdam.de

Accepted 2006 October 20. Received 2006 October 20; in original form 2005 August 23

SUMMARY

Detailed palaeomagnetic investigations were carried out on two 23 m long sediment cores from Erlongwan maar lake, NE China. The sediment composition of both cores is nearly identical. Based on a macroscopical inspection of the cores 410 graded layers intercalated into the laminated sediments were identified. Measurements of the anisotropy of the magnetic susceptibility revealed that these layers have not disturbed the sediment structure in general, but only in intervals where their thicknesses exceeds 50 cm. The age model for Erlongwan is based on 15 AMS ^{14}C-datings on bulk sediment, showing that the sediment profile spans the last 37 ka cal BP. Although one of the sediment cores has been slightly deformed during core recovery, similar inclination and declination records could be obtained by standard palaeomagnetic methods. The stacked inclination and declination records show both variations similar to those known from palaeosecular variation records from Eastern China and Japan. Therefore, the presented study is a contribution to the ongoing process of compiling a PSV mastercurve for East Asia.

Key words: anisotropy of magnetic susceptibility, Erlongwan maar lake, lake sediments, NE China, palaeomagnetism, secular variation.

INTRODUCTION

Magnetostratigraphic investigations on lacustrine sediments are now a common part of studies focusing on the variability of the Earth magnetic field during the past. Despite the limitations of the method given by diagenetic effects alterating the primary magnetic signal, inaccuracy of the chronologies and so on, the geomagnetic palaeosecular variation records (PSV) obtained so far are a useful database for modelling the geomagnetic field behaviour in the last millennia (Korte *et al.* 2005). A lot of work has been done up to now, however, there are still large areas where little information is available. One of these areas is East Asia. During the last decades geomagnetic palaeosecular variation records were obtained from different sites in and around Japan (e.g. Ohno *et al.* 1991, 1993; Ali *et al.* 1999; Hyodo 1999; Yamazaki *et al.* 2003, 1983) providing an excellent database for comparison and correlation. In contrast, palaeomagnetic records from China are sparsely distributed. Records spanning the last up to 70 ka are available from South China (Hyodo *et al.* 1999; Yancheva 2003), Taiwan (Lee *et al.* 1998), the Beijing region (Zhu *et al.* 1994) and the Loess plateau (Zhu *et al.* 2000, 1998). Recently, a group of several small lakes in the Long Gang Volcanic Field (LGVF), NE China, has become the interest of a multidisciplinary investigation as a part of the Asian Lake Drilling project (ALDP) (Yasuda & Catto 2004). Palaeomagnetic investigations were carried out on sediments from two of these lakes. The results presented here were obtained from sediment cores from Erlongwan maar lake (ERL). The sediment profile covers the last 37 ka.

SITE LOCATION AND CORE RECOVERY

The small maar lake Erlongwan (42°18′N, 126°22′E) is a part of the LGVF in NE China (Fig. 1), where basaltic to trachybasaltic volcanic products of quaternary age cover around 1700 km^2 of Archaean basement. The LGVF includes more than 150 cinder cones and eight water filled maar or crater lakes with water depths between 15 and 127 m (Mingram *et al.* 2004). The last known volcanic activity occurred around 1600 BP (Fan *et al.* 2000). The ERL lies 724 m above sea level within the Archaean basement. The lake has a water depth of 36 m, a surface area of 0.3 km^2 and a catchment area of 0.4 km^2. The rocks in the catchment area of the lake are composed of gneiss, amphibolite and magnetite bearing quartzite from the Anshan Migmatite group (Geological Survey of Jilin 1994).

Two sediment cores, 24.4 and 23.3 m long, were recovered from the deepest part of ERL in 2001 (Fig. 1), using a raft-operated Usinger piston corer (a modified Livingston piston corer, Usinger 1991). The individual core sections are 2 m long with a diameter of 80 mm down to around 16 m (ERL-A) and 15 m sediment depth

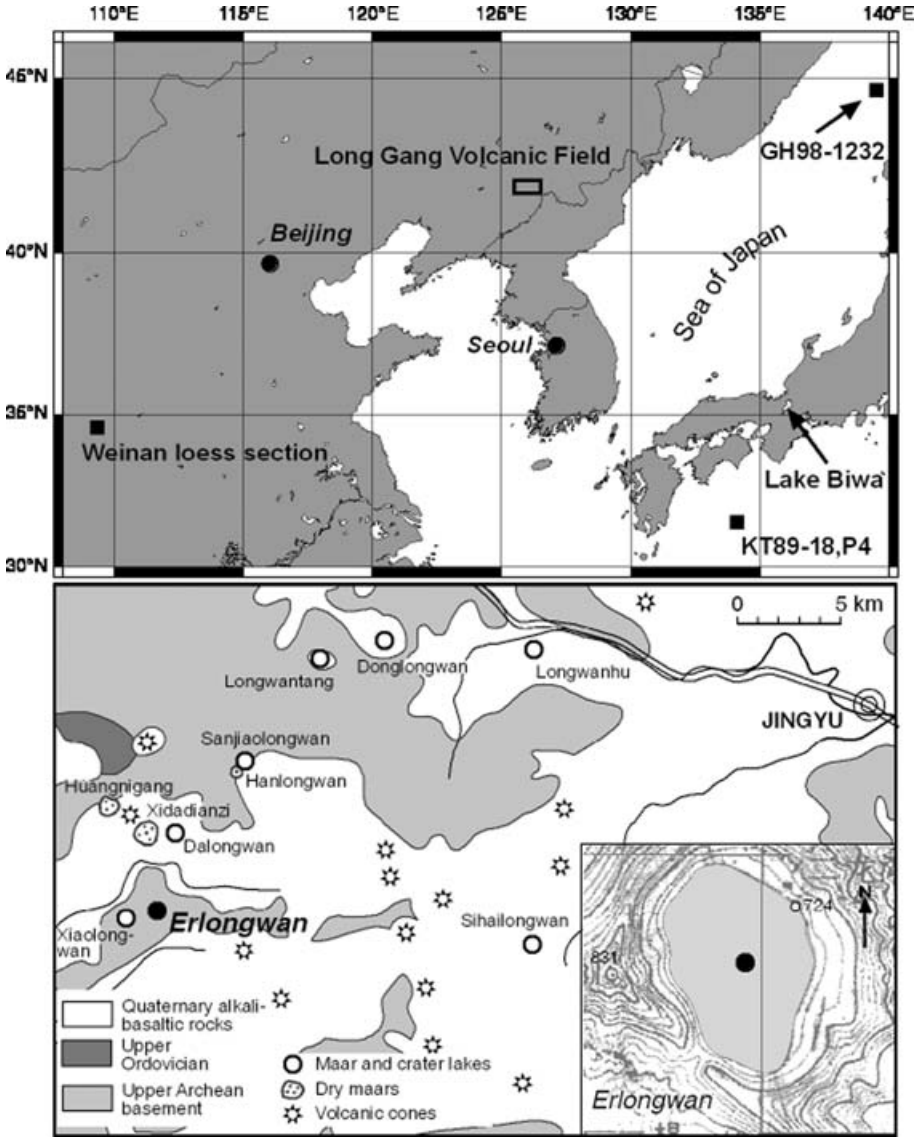

Figure 1. Location and simplified geological map of the Long Gang Volcanic Field (LGVF). Lake Erlongwan is situated in the western part of the LGVF. The coring location is marked by a dot on the topographical map of the lake area. The locations referred to in the text are marked by black squares on the geographical map.

(ERL-B), respectively. Below this depth the diameter of the cores is 55 mm. The lowermost individual core section from core ERL-A with a diameter of 40 mm and a length of 0.98 m was not available for subsampling.

METHODS

Directly after arrival at the GFZ Potsdam the cores were opened, cut into 1 m segments and split into halves. They were than sealed in polythene and cold stored. On the split halves of the cores continuous high resolution logs of magnetic susceptibility were measured with a Bartington MS2E spot reading sensor integrated in an automated core logging system in steps of 1 mm. The cores were subsampled with cubic plastic boxes ($20 \times 20 \times 15.5$ mm) that were pushed into the surface of the core halves in sampling intervals of 20 mm. For a more detailed description of the sampling method used see Frank (2007). A total of 943 and 947 samples were derived from cores ERL-A and ERL-B, respectively. Intervals composed of coarse-grained material and plant remains, that are the graded layers (GRLs) with thicknesses exceeding 50 cm, were not subsampled, except for one pilot layer. All samples were weighted in order to get initial information on the variations in sediment composition. For the determination of the anisotropy ellipsoid of the magnetic susceptibility (AMS) of the subsamples, a Kappabridge KLY-3S (AGICO Brno) was used. Calculation of the anisotropy tensor as represented by the general susceptibilities K_{max} (maximum), K_{int} (intermediate) and K_{min} (minimum), as well as their respective orientation angles was done with AGICO software.

Directions and intensities of the natural remanent magnetisation (NRM) were measured with a fully automated 2G-755-Superconducting Rock Magnetometer (SRM) based on DC-SQUIDS with a noise level less than 10^{-6} Am^{-1} related to a sample volume of 6.2 cm^3. NRM intensities of the investigated cores range between 10^{-3} and 10^{-1} A m^{-1}. The stability of the NRM was tested by alternating field (AF) demagnetisation which was carried out in 10 steps of up to 100 mT using the integrated

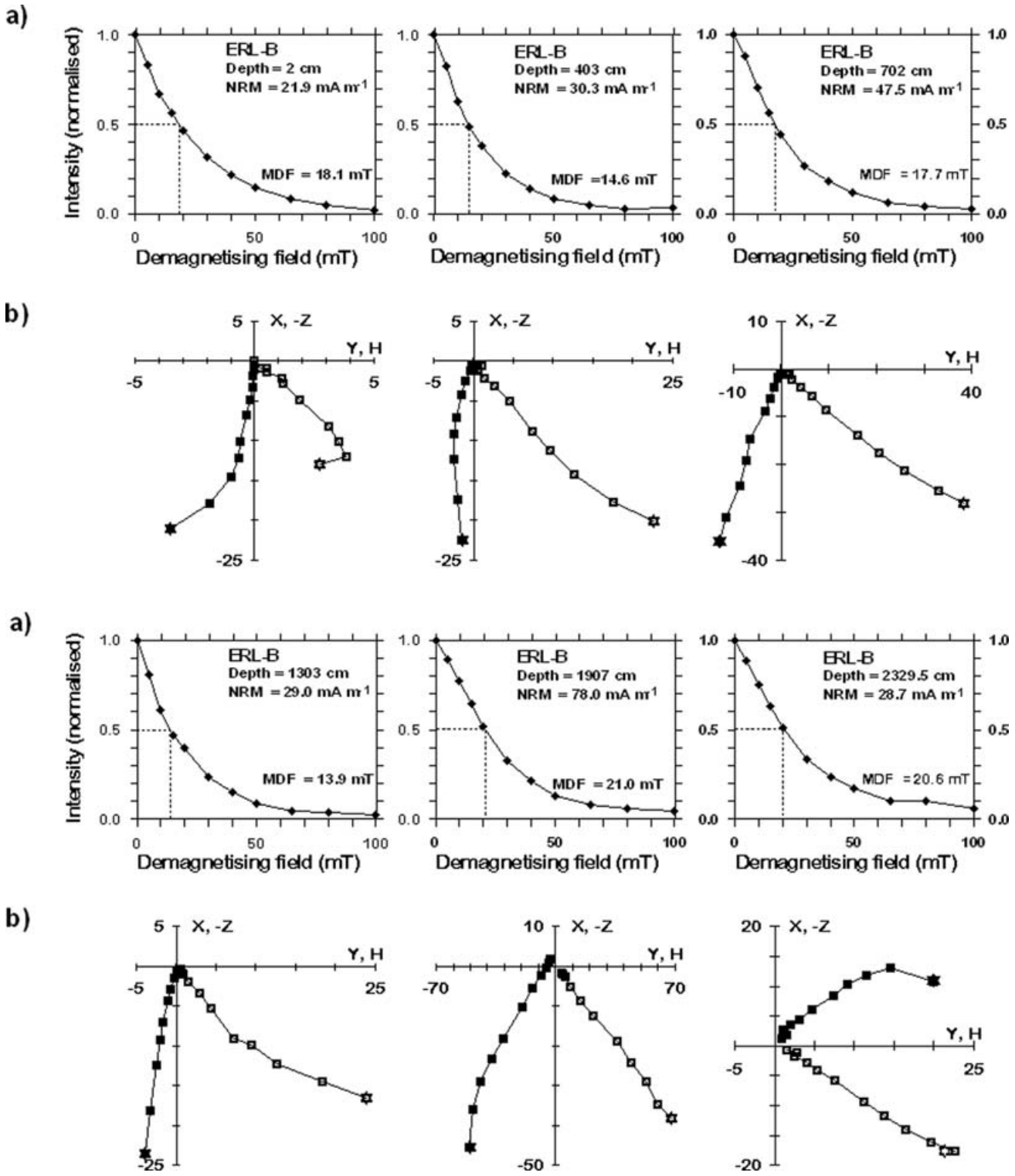

Figure 2. Results of the alternating field demagnetization of six samples from core ERL-B from Erlongwan maar lake. (a) Normalised NRM intensity versus AF peak amplitudes. Sampling depth, NRM intensity, and median destructive field (MDF) of each sample are indicated in the plots of the demagnetisation curves. (b) Orthogonal projections (Zijderveld diagrams) of the stepwise demagnetisation of the same samples. Demagnetisation steps run from 0 to 100 mT. The units are 10^{-3} A m^{-1}. Closed symbols denote X plotted versus Y, and open symbols denote Z plotted versus H. The NRM measurement in each curve is marked with an asterisk.

in-line three-axis AF demagnetiser of the cryogenic-magnetometer. Typical demagnetisation curves and the orthogonal demagnetisation (Zijderveld) diagrams show that a secondary viscous remanent magnetisation (VRM) is progressively destroyed from 5 to 15 mT (Fig. 2). Further steps revealed a high stability of the magnetisation directions.

The directions of the characteristic remanent magnetization (ChRM) were derived from principle component analysis

(Kirschvink 1980) of the results of successive demagnetization steps. The demagnetization steps from 0 (NRM) to 10 mT as well as those from 65 to 100 mT were excluded from the vector analysis. Since the cores were obtained without azimuthal orientation, the mean ChRM-declination value of the top core sections, ERL-A 1u and ERL-B 1o, were set to zero. Afterwards the remaining core sections were also rotated, fitting the ends of the individual declination logs together. The obtained ChRM-inclination and declination profiles were transformed to a common depth scale and subjected to palaeomagnetic pattern matching. The vast majority of the section boundaries in the ERL cores are situated at different stratigraphic depths, providing a good control for this declination adjustment technique.

RESULTS AND DISCUSSION

Sediment composition

The sediments from ERL have an organic to minerogenic composition and are laminated throughout the whole profile. A total of 410 GRLs with thicknesses ranging from 0.1 to 150 cm are intercalated into the sediment sequence. The microscopically analysis of thin sections revealed that the mineralogical composition of the GRLs did not differ from the minerogenic components in the laminated sediment sections. The lithological profile for the sediment cores from Erlongwan maar lake is based on visual inspection of the sediments (J. Mingram, personal communication, 2003) (Fig. 3). It was refined by the results of sedimentological and geochemical analysis which will be published elsewhere. The only sedimentological parameter presented here is the density of the wet samples which reflects an increase in the content of minerogenic material from top to bottom of the profile (Fig. 3) as well as the increase in compaction of the sediments with depths. The transition from an organic-minerogenic to a minerogenic-organic sediment composition at 632 cm depth is interpreted as the Holocene/Pleistocene boundary. It is marked by a distinct increase in the wet density of the samples (Fig. 3). Below this boundary the wet density values are nearly constant with values between 1.5 and 1.7 g cm^{-3}. Above 632 cm, in the organic rich sediments, the wet density is distinctively lower and varies between 1.1 and 1.4 (Fig. 3). Two intervals

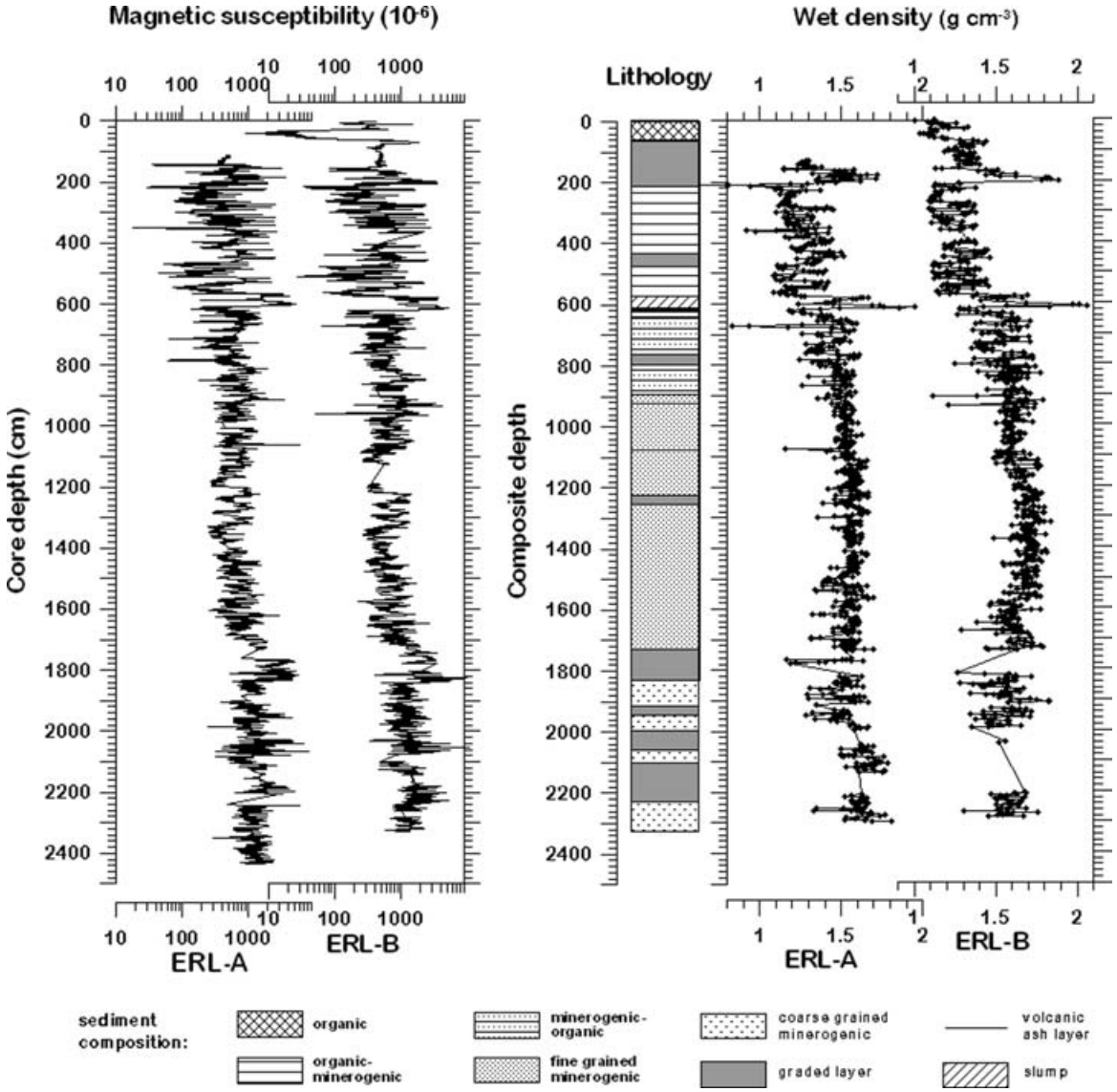

Figure 3. High-resolution logs of the magnetic susceptibility of cores ERL-A and ERL-B versus individual core depth (left) and wet density records for the same cores versus composite depth including a lithological column (right).

with increased wet density values are linked to the coarse-grained bottom of a thick GRL (160–210 cm) and to a slump bearing a volcanic ash layer (560–620 cm), respectively. Higher wet densities and peaks in the continuous high resolution records of the magnetic susceptibility in the topmost 632 cm are always linked to the occurrence of GRLs with thicknesses >1 cm, which is more than half of the respective sample (Fig. 3). Below 910 cm depth, in the minerogenic part of the sediments, the contrast in the amount of clastic material in the bulk sediment compared to a GRL is too low to be reflected in susceptibility or dry density records. An exception comprises the thick GRLs in the lowermost 6 m of the profiles.

The coring positions of ERL-A and ERL-B lay only some metres apart, and the core photographs reveal an identical succession of laminated sequences and GRLs in both cores. Nevertheless, below 700 cm depth the wet density record of ERL-B shows much more variability and higher mean values compared to ERL-A (Fig. 3). This effect must probably be attributed to the more pronounced sediment deformation in core ERL-B compared to ERL-A (see also Fig. 6), originating from the coring process.

Correlation and chronology

The correlation between the two cores from ERL is based on visual inspection of the cores, using the 410 GRLs as marker layers. Additionally, a peak-to-peak correlation based on the high resolution logs of magnetic susceptibility was possible for the greater part of the profile (Fig. 3). Only the thick GRLs (>50 cm) show no correlatable internal susceptibility features in both cores. Based on the macroscopical inspection of the cores (J. Mingram, personal communication, 2003), a composite profile comprising a continuous sedimentary record was compiled by adding and/or replace missing or disturbed parts of the sediment core ERL-B with segments from core ERL-A. This compilation was later improved by the results of core correlation by rock magnetic means. The depths of ERL-A and ERL-B were transformed into a composite depth scale, which will be referred to throughout the whole text.

The chronology is based on 15 AMS radiocarbon dating of bulk sediment samples taken from the fine laminated sediment sections (Table 1, Fig. 4). The content of inorganic carbon in these samples is below 0.1 wt %, indicating that there is no hard water effect. The dating was done at Poznan Radiocarbon laboratory (http://www.radiocarbon.pl). The ^{14}C ages were calibrated with the calibration programs IntCal04 (Reimer *et al.* 2004) for ages younger than 22 ka and CalPal (http://www.calpal-online.de) for ^{14}C ages older than 22 ka. It was assumed that the GRLs formed within a few years only, as a result of events with increased precipitation. Thus all GRLs were excluded from the depth-age calculation before interpolating between the available ^{14}C ages. This might cause a numerical error because the sediments in the thicker layers will not be settled within 1 or 2 yr. However, this error is negligible compared to the dating error for the calibrated ^{14}C ages in general (Fig. 4). The calculated mean sedimentation rate for the sediments younger than 31 ka is 0.27 mm a^{-1}, which is 74 yr within one sample. Sediments older than 31 ka, that is, the coarse-grained minerogenic sediments, have a lower mean sedimentation rate of 0.20 mm a^{-1}.

Magnetic susceptibility and natural remanent magnetization

The patterns of NRM intensity (J_{NRM}) of the cores investigated are very similar to those of the corresponding susceptibility profiles (Figs 5a and b). Both NRM and κ_{LF} logs from ERL-A and ERL-B are dominated by a succession of distinct peaks which reflect the presence of graded layers, especially in the uppermost 800 ($\kappa_{LF)}$ to 1000 cm (NRM) and below 1700 cm depth. In these layers J_{NRM} is up to 10 times higher reaching values of up to 600 mA m^{-1} whereas in the organic–minerogenic to fine-grained minerogenic sediments the mean value is 40 mA m^{-1}. The more spiky nature of the NRM records is probably due to the higher sensitivity of the NRM with regard to grain size variations. Detailed rock magnetic investigations including high temperature measurements of the saturation magnetization revealed, that magnetite in the pseudo-single-domain range is the dominant carrier of the magnetic remanence in the Erlongwan sediments (Frank 2007). The topmost 60 cm of the profile, consisting of laminated organic sediments, are characterized by low susceptibilities and NRM intensities, due to a reduced input of minerogenic material. Higher J_{NRM} and κ_{LF} values within

Table 1: AMS ^{14}C-dates measured on bulk sediment

Lab.-#	Composite depth (cm) mean value	^{14}C age (BP)	calibrated age BP (2σ 95% prob.)
Poz-11744	44.0	545 ± 30	515 – 652
Poz-10988	264.6	2865 ± 30	2917 – 3076
Poz-11746	413.2	6200 ± 40	6994 – 7128
Poz-11004	503.8	7760 ± 40	8433 – 8600
Poz-11743	624.0	9650 ± 50	10785 – 10979
Poz-11747	799.2	13470 ± 70	15630 – 16437
Poz-11044	918.7	14180 ± 70	16488 – 17345
Poz-11749	1068.7	16230 ± 70	19192 – 19511
Poz-11750	1176.4	18400 ± 90	21446 – 22230
Poz-11751	1370.0	20980 ± 120	24777 – 25589
Poz-11045	1464	22340 ± 150	26540 – 27359
Poz-10919	1586	23040 ± 140	26540 – 27768
Poz-11752	1710.0	26960 ± 200	30990 – 31694
Poz-11005	1990	28750 ± 250	32313 – 35070
Poz-1175346	2280.4	32180 ± 360	36152 – 38817

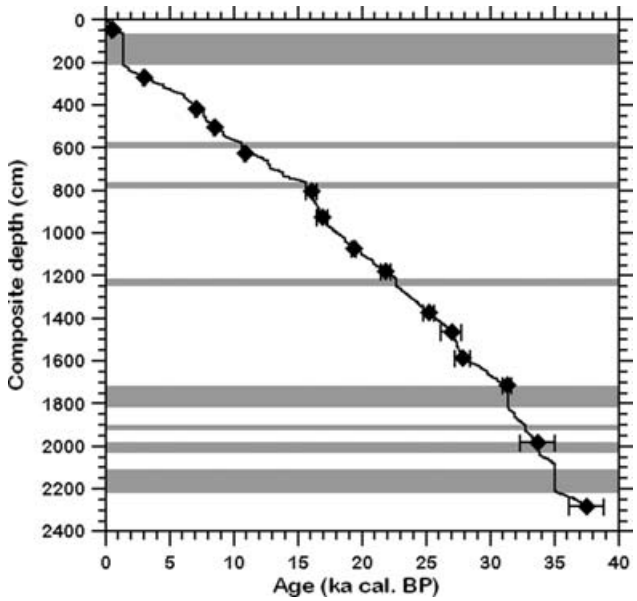

Figure 4. Depth/age model for the Erlongwan maar lake profile based on 15 calibrated AMS ^{14}C-ages (Table 1). Error bars for the younger radiocarbon dates are smaller than the size of the symbol. The grey shaded areas denote thick GRLs. For more details see text.

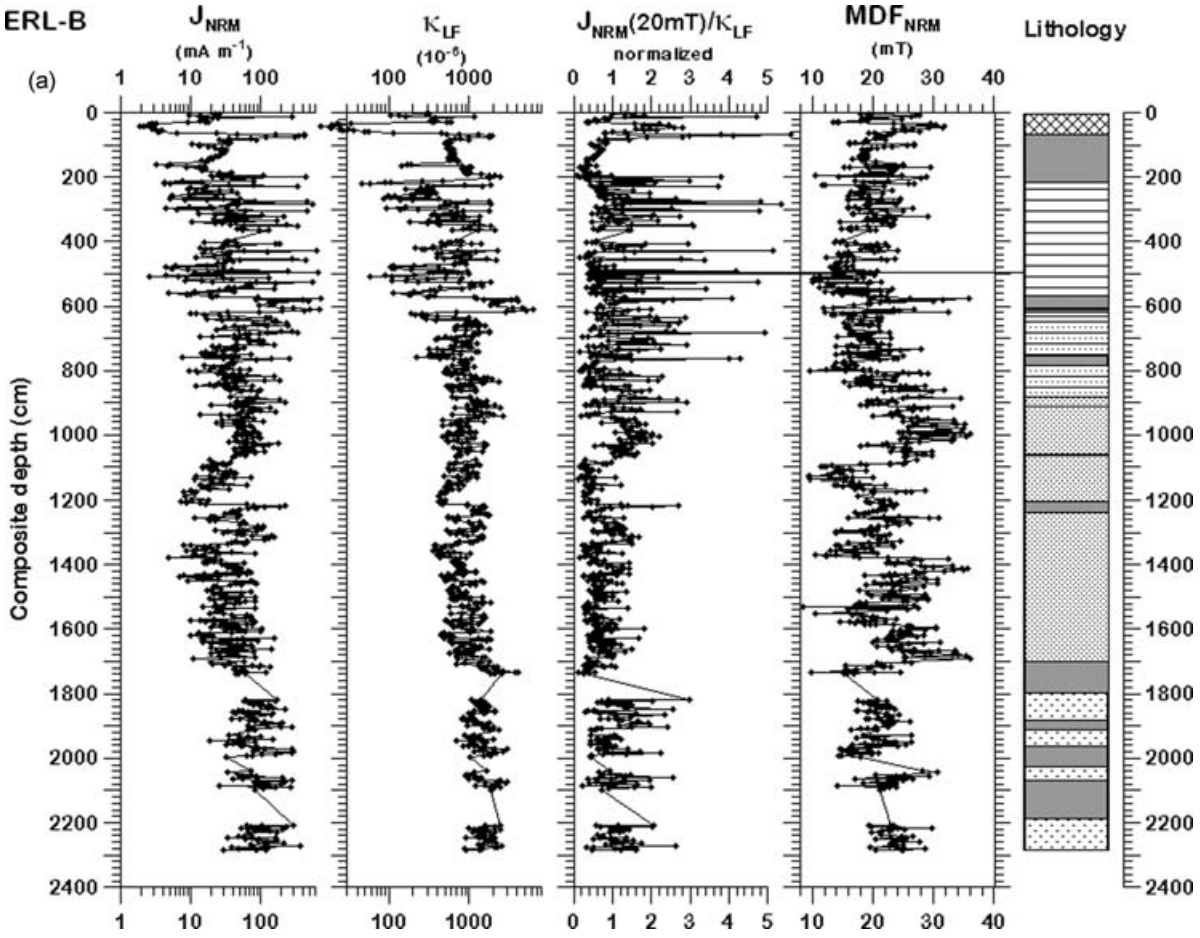

Figure 5. Downcore logs of NRM-intensity (J_{NRM}), magnetic susceptibility (κ_{LF}), ratio of $J_{NRM/}\kappa_{LF}$ after demagnetisation at 20 mT, median destructive field of the NRM (MDF_{NRM}) and lithology versus composite depth for (a) core ERL-B and (b) core ERL-A. The legend for the lithology is given in Fig. 3.

this interval are again linked to a GRL between 12.2 and 30.9 cm depth (Fig. 5a). The transition from organic to organic–minerogenic sediments at 632 cm depth is well reflected in both, susceptibility and NRM intensity, records. It is overlain by a small slump including a volcanic ash layer, associated with a tenfold increase of J_{NRM} and κ_{LF} when compared to the sections directly below and above (Figs 5a and b). Below 1700 cm depth, in the coarse-grained minerogenic sediment, the content of magnetic minerals slightly increases.

Considering the great variability in J_{NRM} it is doubtful that the ERL sediments could be used for a reconstruction of the intensity variations of the geomagnetic field. Nevertheless, the relative palaeointensity of the geomagnetic field was estimated by normalizing the NRM-intensities after demagnetization at 20 mT [J_{NRM} (20 mT)] by κ_{LF} (Figs 5a and b). The resulting records still show the spiky nature of the NRM intensity, indicating that the contribution of the geomagnetic palaeofield to the NRM intensity is still veiled by the large variations in the grain size of the magnetic particles. The high variability in grain size is also reflected in the median destructive field of the NRM (MDF_{NRM}), which could be interpreted as an grain size indicative parameter, due to the almost monomineralic composition of the magnetic carrier fraction as was revealed by detailed rock magnetic investigations (Frank 2007).

Anisotropy of magnetic susceptibility and directions

In order to judge on the reliability of the magnetic signal stored, with regard to the numerous GRLs intercalated into the sediment sequence, detailed information about the magnetic fabric of the sediments was needed. Additionally, mechanical disturbances due to drilling and recovery of the cores could have a strong impact on the sediment fabric. Deformation of the sediments should be reflected by the shape parameter q and in the inclination of K_{min} with $q = (K_{max} - K_{int})/[(K_{max} + K_{int})/2 - K_{min}]$ (Granar 1958). Following Tarling & Hrouda (1993) the primary fabric of the sediment ideally correspond to a foliated ellipsoid with $0.06 < q < 0.67$ and the directions of K_{min} lying within 20° of the vertical of the bedding plane. According to this criteria only the samples from the thick GRLs (>50 cm) and a minor amount of single samples from ERL-A were rejected. The latter are related to a volcanic ash layer at 620 cm depth (Fig. 5b) and lithic fragments. In contrast, there are several deformed sediment sequences in core ERL-B, confirmed by the core photographs. The most prominent are between 800 and 850 cm and 1090–1170 cm (Fig. 6). Single samples with deviating inclinations of K_{min} related to lithic fragments, volcanic ash layers and thick GRL are visible in this core too. In both cores the GRLs with thicknesses <50 cm show no higher degree of anisotropy. Apparently there is no difference in the sedimentation mechanism of

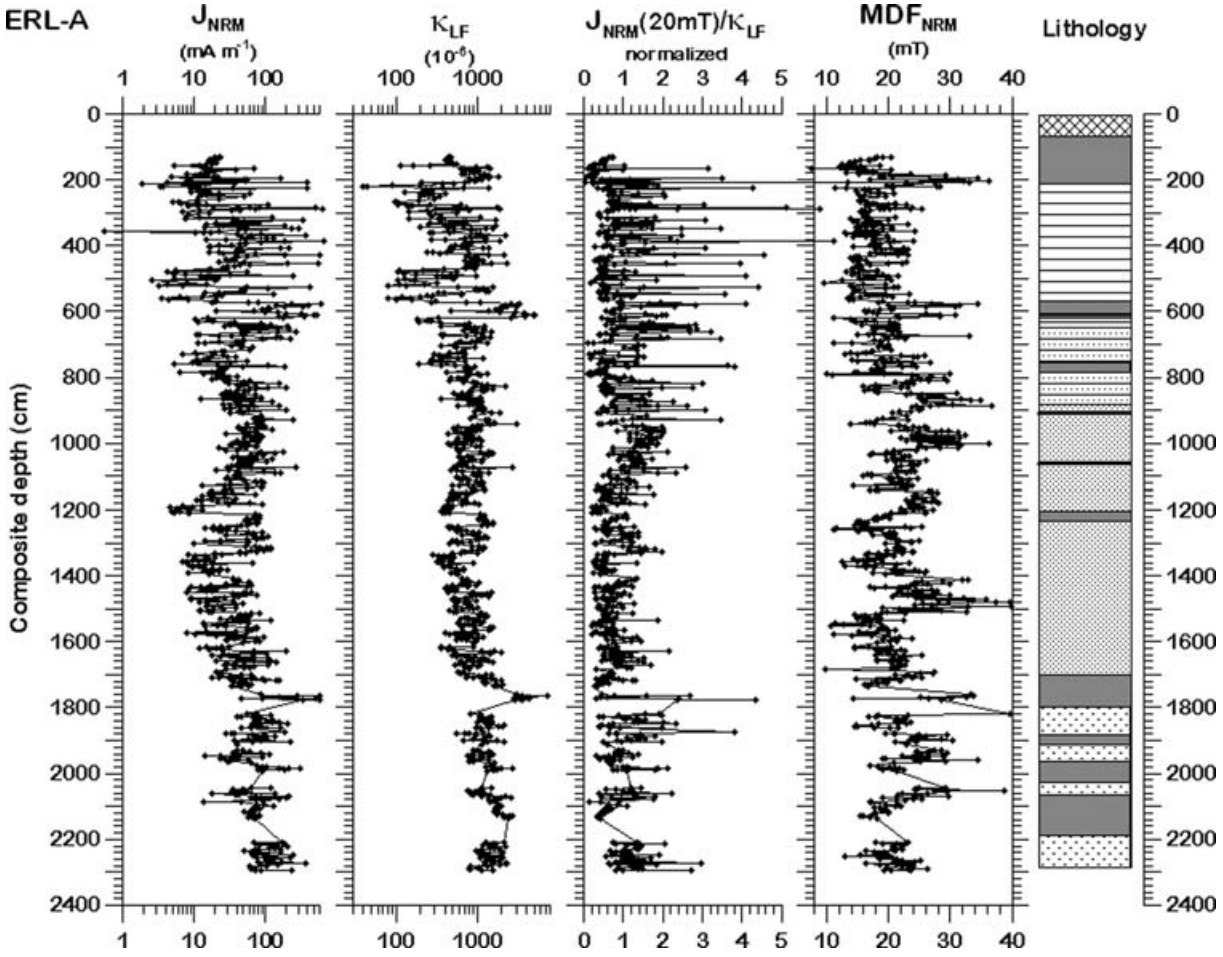

Figure 5. (*Continued.*)

material (clastic, organic) washed into the lake periodically or within flood events caused by heavy rains or strong melt water events. Therefore, it can be concluded, that the increase in the degree of anisotropy is caused by (1) a coarsening of the grain size linked to the bottom part of a thick GRL and (2) the inhomogeneous composition of this sections including a lot of terrestrial plant remains. The deformation of the sediments due to core recovery by a piston corer is visible in form of a slight flattening of the inclination of $K_{\min}$ at the boundaries of the 2 m core sections (Fig. 7.) This effect is more pronounced in the record from ERL-B, indicating again, that this core was stronger affected by the coring procedure than ERL-A.

A direct comparison between the ChRM-inclination (I_{CHRM}) and the inclination of $K_{\min}$($I_{K\min}$) revealed that the sediment deformation has clearly affected the directional signal of the geomagnetic field within several intervals in ERL-B (Fig. 7). These are the sections were massive core deformation occurred, that is between 800 and 850 cm and 1080–1170 cm. The samples from the organic sediment at the top of the core and from the underlying GRL show anomalous high ChRM-inclinations (Fig. 7). However, in other, often thinner intervals, that is, around 600 cm and between 1580 and 1700 cm in core ERL-B, there is no correspondence at all between I_{CHRM} and $I_{K\min}$. Rosenbaum *et al.* (2000) demonstrated that there is no clear relation between the two inclinations regarding a single sample and deformation will not produce a simple relation between the orientation of the palaeomagnetic directions and $K_{\max}$, $K_{\min}$ and K_{int}. Therefore, it is not possible to correct the palaeomagnetic directions of the single samples by means of anisotropy measurements.

Because of the unique possibility to compare results for two cores with nearly identical sedimentology but different degree of deformation, the influence of the anisotropy of the sediment fabric on the ChRM-inclinations could be quantified for the sediments from Erlongwan (Fig. 7). It was assumed, that in intervals without sediment deformation, expressed either as a flattening of $K_{\min}$ or by $q <$ 0.2, the recorded variations of ChRM correspond to true variations of the Earth magnetic field vector. The inclination record from core ERL-A which is characterized by a lower degree of deformation, was chosen as the reference curve for the Erlongwan site. All features in ERL-B that correspond to those in ERL-A were then assumed to have recorded true features of the geomagnetic field, despite any observable flattening of $K_{\min}$. In ERL-B there are two depth intervals where such conclusion could be drawn, that is, between 800 and 850 cm and 1600–1700 cm depth, respectively (Fig. 7). In the deeper interval the shape of the inclination curve in both cores is similar although the data in ERL-B is more scattered. Between 800 and 850 cm there is an inclination high that is present in both records, possibly indicating a real variation in the direction of the geomagnetic field vector. It must be considered however, that this interval is dominated by two GRL, so it spans only a short-time interval. In general, there is no connection between GRLs and a steeping of the ChRM-inclination (Fig. 7).

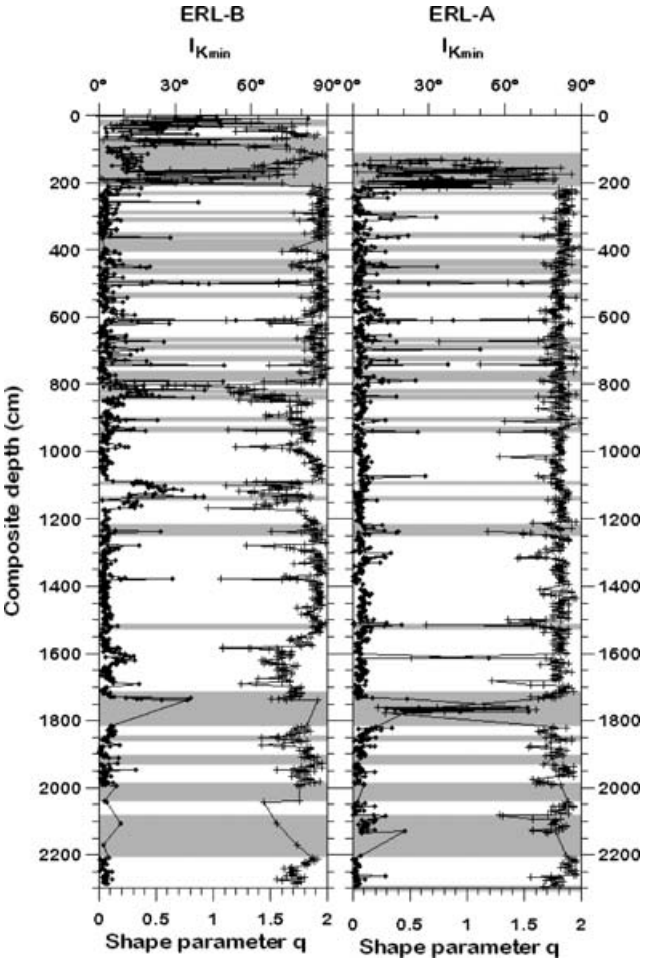

Figure 6. Results of the measurement of anisotropy of the magnetic susceptibility: Records of the shape parameter q (diamonds) and the inclination of $K_{\min}$ (crosses) versus composite depth for core ERL-B (left) and ERL-A (right). $q = (K_{\max} - K_{\text{int}})/[(K_{\max} + K_{\text{int}})/2 - K_{\min}]$. The grey shaded areas mark graded layers >10 cm.

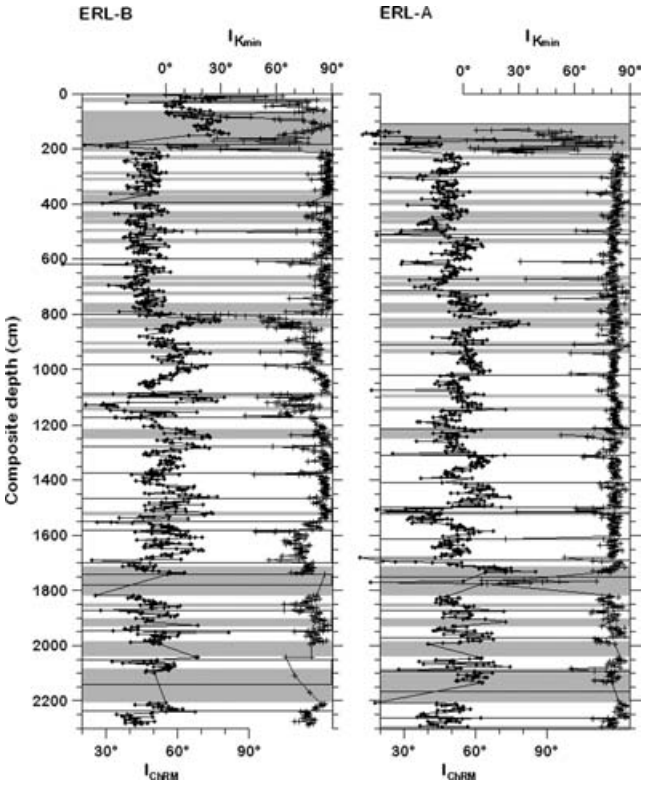

Figure 7. Comparison of the ChRM-inclination records with the inclination of $K_{\min}$ for core ERL-B (left) and ERL-A (right). The grey shaded areas mark graded layers >10 cm. The black lines denote the boundaries of the single cores sections.

The outlier corrected ChRM-inclination and declination records from ERL-A and ERL-B are shown in Fig. 8. There is a general agreement between the succession of highs and lows in both inclination records, although the amplitudes are different. The mean inclination of 50° is lower than the expected dipole inclination of 61° for this site. The reasons for this commonly observed inclination shallowing in sediments can be manifold (e.g. Arason & Levi 1990a; Lu *et al.* 1990; King & Channell 1991), the existence of the GRLs however, did not contribute apparently. Most of these layers are thinner than 5 cm, and there is no reason to assume that the sedimentation mechanism, that is, downward movement of the magnetic particles through the water column, in these layers differs significantly from those of the under and overlaying laminated sediments. There is no explanation for the observed smoothing of the inclination record from ERL-B between 450 and 700 cm, compared to ERL-A. There is neither a difference in the sedimentation rate nor is this sequence deformed (Figs 6 and 7).

The agreement between the declination records is much better, which is partly an artefact of the palaeomagnetic pattern matching method (Fig. 8). The variations are in the range of ±30°, which is typical for geomagnetic palaeosecular variations. Whether the prominent westward swing in declination between 700 and 400 cm

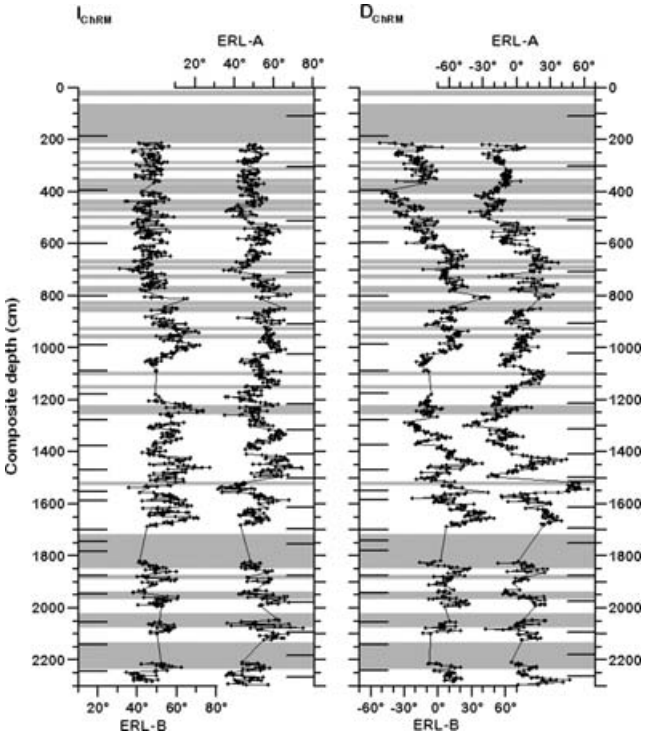

Figure 8. Comparison between the outlier corrected ChRM-inclination and declination records obtained from cores ERL-B and ERL-A versus composite depth. The grey shaded areas mark graded layers >10 cm. The short black lines denote the boundaries of the single cores.

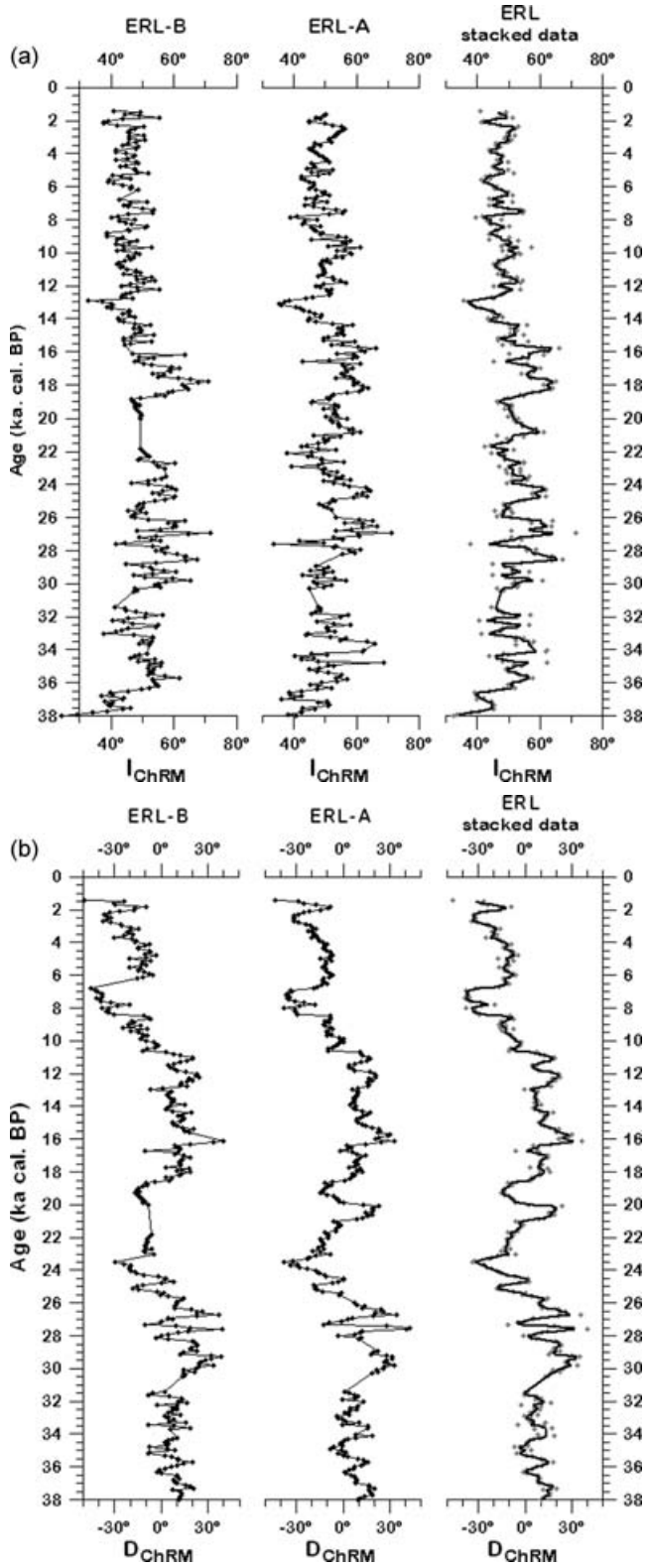

Figure 9. Stacked ChRM-inclination (a) and ChRM-declination records (b) for Erlongwan maar lake versus age (grey diamonds). The records were smoothed with a weighted three-point-running-average (black line). Additionally, the individual core records are shown versus age.

depth is a true feature of the geomagnetic field has to be tested by comparison with other PSV records from the region.

In order to obtain representative ChRM-inclination and declination curves for the Erlongwan site, the records derived from cores ERL-A and ERL-B were transformed into time-series using the age model presented in Fig. 4 and numerical resampled in 100 yr intervals. Due to this resampling method there is nearly none contribution of the GRLs to the ChRM-inclination and declination records. These data sets were then stacked by calculating the mean inclination and declination for each time level (Figs 9a and b). The remaining high frequency component of the stacked records was filtered with a weighted three point-running-average.

Regional comparison

Regional comparison was performed with two marine records, core GH98-1232 from the Japan Sea (Yamazaki *et al.* 2003) and core KT89-18, P14 from Off Shikoku, SW Japan (Ohno *et al.* 1993) and one terrestrial record from the Weinan loess section in China (Zhu *et al.* 1999) (Figs 1, 10a and b). All records are presented versus their uncalibrated ^{14}C-ages, as given in the related publications. Corresponding features are marked by letters, those for the inclination records are taken from Yamazaki *et al.* (2003). For the interpretation of the results it should be considered, that (1) the time resolution of the marine and loess records is lower compared to the Erlongwan profile and (2) the presented records are based on one core from each site only (Ohno *et al.* 1993; Yamazaki *et al.* 2003; Zhu *et al.* 1999).

Within this limits there is an agreement between all four records, allowing for identification of a number of pronounced inclination lows in the time interval 0–25 ka (Figs 10a and b). For the sediments older than 25 ka correlation with the ERL records is of a more speculative nature due to the thick GRLs that are intercalated into the lowermost 6 m of the profile (Fig. 7). It is remarkable however, that most of the high frequency features of the inclination record of ERL could be identified at least in one of the two marine records. The lower amplitudes in the latter are due to their lower sedimentation rates, which are in the range of 0.2 mm a^{-1} (Off Shikoku, SW Japan) and 0.15 mm a^{-1} (Japan Sea), respectively. The minor divergences in the ages of the correlatable features between the records presented could be attributed to dating errors.

There are fewer features in the declination records presented that could be identified in all four records (Fig. 10b). The records from around Japan and Erlongwan look most similar in the time interval 0–10 ka, that is, the Holocene. The pronounced westward deflection of the field vector at the ERL site between 12 and 5 ka is not recorded in any of the other records and is probably an artefact of the declination adjustment technique used. Most of the overlying high frequency variations, however, could be identified in one of the two marine records (Fig. 10b) at least. The inclination and declination records from the Weinan Loess section are more similar to those of the ERL records concerning the shape and amplitudes of the low frequent variations than to the marine records.

A comparison between the Holocene part of the stacked inclination and declination records from ERL and those from Lake Biwa (Ali *et al.* 1999) is shown in Figs 11(a) and (b). All records are shown versus their calibrated ^{14}C-ages. The correlatable features are marked by letters corresponding to those in Figs 10(a) and (b). The most prominent features in both records are an inclination minimum dated around 8 ka cal PB (Fig. 11a) and a westward deflection in the declination between 4 and 3.2 ka cal PB (Fig. 11b). The latter

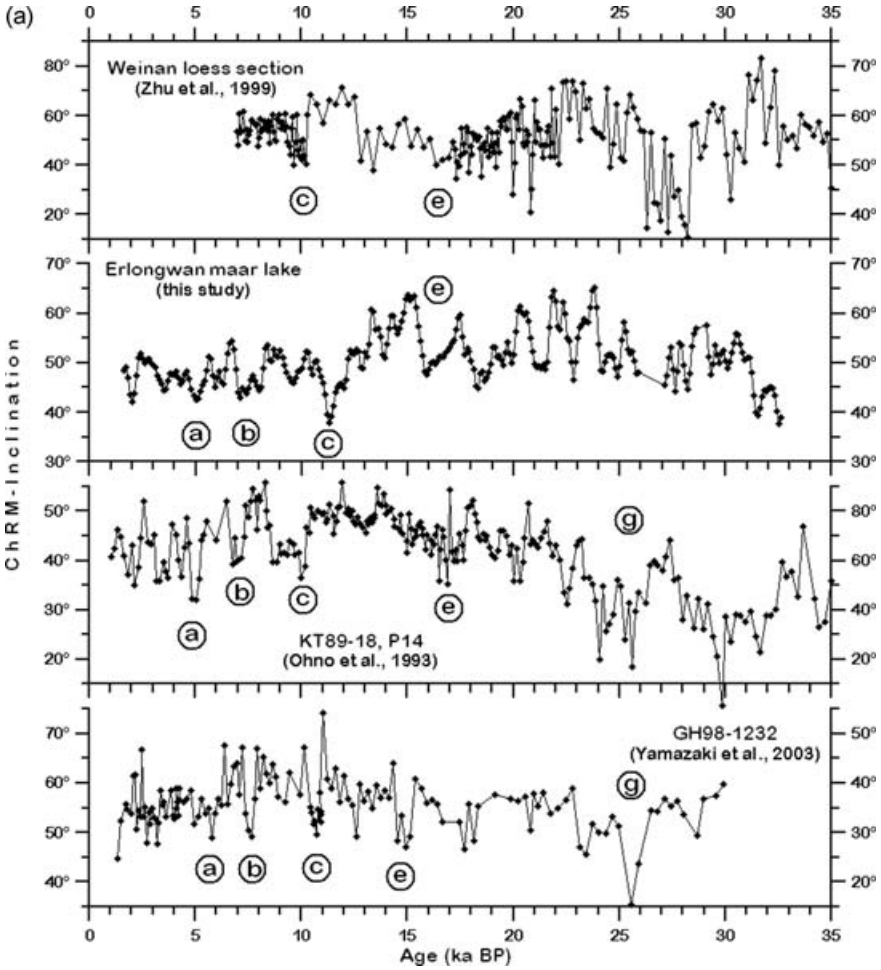

Figure 10. Comparison of inclination (a) and declination records (b) from core GH98-1232 from the Japan Sea (Yamazaki *et al.* 2003), core KT89-18, P14 from Off Shikoku, SW Japan (Ohno *et al.* 1993) and a record from the Weinan loess section in China (Zhu *et al.* 1999) with the palaeomagnetic records from Erlongwan maar lake. All records are presented versus their uncalibrated ^{14}C-ages. The geographical position of all sites is given in Fig. 1. The correlatable features are marked by letters.

is also known from Europe and North America and was interpreted as a feature of a westward drifting non-dipole field with a rate of about 0.13° a^{-1} (Hyodo *et al.* 1993). The correspondence in the shape of both inclination and declination curves is quite good, although most of the low frequency variations in the Biwa records are missing in ERL. This is mainly due to differences in sedimentation rate which is five times lower in the ERL-sediments compared to Lake Biwa (Ali *et al.* 1999). Nevertheless, the overall agreement in the presented PSV records confirms that the sediments from Lake Erlongwan are reliable recorders of the Earth's magnetic field variations on a millennial timescale for the last 20 ka at least.

CONCLUSIONS

The detailed palaeomagnetic study carried out on two 23 m long sediment cores from Erlongwan maar lake, NE China, yielded inclination and declination records which look similar to PSV records already published for Northeast Asia. The intersite correlation also confirmed that most of the high frequency variations stored in the ERL sediments are of geomagnetic origin, reflecting variations in the Earth magnetic field vector during the last 37 ka cal BP. The occurrence of GRLs, especially those with thickness <50 cm has not influenced the structure of the sediment significantly, as was obtained from the measurement of the anisotropy of the magnetic susceptibility. Sediment deformations produced by the coring methods used have had a greater impact on the recorded directional variations of the geomagnetic field. A hint on the very complex process of remanent acquisition in laminated lake sediments is given by the observed differences in amplitude between the ChRM records from cores ERL-A and ERL-B, despite their identical sediment composition. The results of this study contribute to the ongoing process of compiling a PSV mastercurve for East Asia.

ACKNOWLEDGMENTS

The author would like to thank J. Mingram, D. Berger, M. Köhler, D. Acksel, H. Howey and I. Heymann for coring. M. Haack, D. Sonnabend and C. Schmeltzer helped during laboratory work. T. Yamazaki and R. Zhou are kindly acknowledged for providing their data. G. Yancheva critically reviewed an early version of this paper. Two anonymous reviewers are acknowledged for their critical comments. This study was funded by the German Research Foundation (DFG), grant Fr1672/1-1.

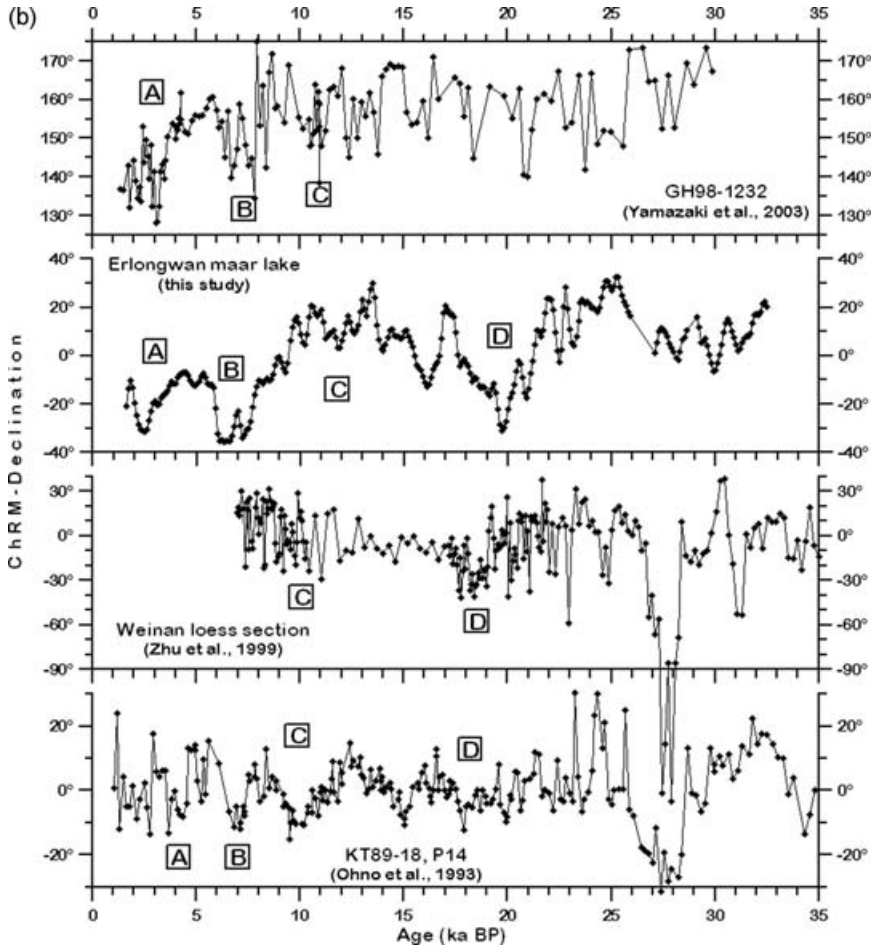

Figure 10. (*Continued.*)

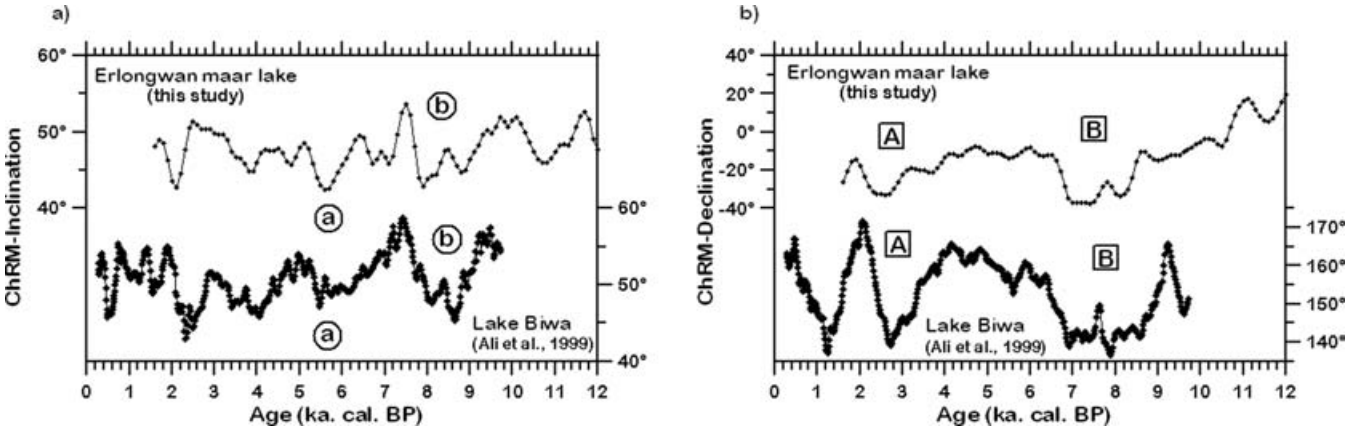

Figure 11. Comparison of the stacked inclination and declination records from Erlongwan maar lake with the Holocene records from Lake Biwa (Ali *et al.* 1999). The letters denoting the correlatable features are the same as in Fig. 10. Both records are presented versus their calibrated ^{14}C-ages.

REFERENCES

Ali, M., Oda, H., Hayashida, A., Takemura, K. & Torii, M., 1999. Holocene palaeomagnetic secular variation at Lake Biwa, central Japan, *Geophys. J. Int.,* **136,** 218–228.

Arason, P. & Levi, S., 1990a. Models of inclination shallowing during sediment compaction, *J. geophys. Res.,* **95,** 4481–4499.

Fan, Q., Sui, J., Liu, R., Wei, H. & Li, N., 2000. Petrology and geochemistry of Jinlongelingzi active volcano – the most recent basaltic volcano at Longgang, *Chinese J. Geochem.,* **19,** 312–317.

Frank, U., 2007. Rock magnetic studies on sediments from Erlongwan maar lake, Long Gang Volcanic Field, Jilin province, NE China, *Geophys. J. Int.,* **168,** 13–26.

Granar, L., 1958. Magnetic measurements on Swedish varved sediments, *Artiv. f. Geofysik,* **3,** 1–40.

Geological Survey of Jilin, 1994. *Geology of Jilin, China* (in Chinese), Geological Publishing House, Beijing.

Hyodo, M., 1999. Recent progress in paleomagnetic and rock-magnetic studies of the Quaternary in Japan, *Quater. Res.,* **38,** 202–208.

Hyodo, M., Itota, C. & Yaskawa, K., 1993. Geomagnetic secular variation

reconstructed from magnetizations of wide-diameter cores of Holocene sediments in Japan, *J. Geomag. geoelectr.,* **45,** 669–696.

Hyodo, M. *et al.*, 1999. A late Holocene geomagnetic secular variation record from Erhai Lake, southwest China, *Geophys. J. Int.,* **136,** 784–790.

King, J.W. & Channell, J.E.T., 1991. Sedimentary magnetism, environmental magnetism and magnetostratigraphy, *Rev. Geophys., Suppl.,* **29,** 358–370.

Kirschvink, J.L., 1980. The least-squares line and plane and the analysis of palaeomagnetic data, *Geophys. J. R. astr. Soc.,* **62,** 699–718.

Korte, M., Genevey, A., Constable, C., Frank, U. & Schnepp, E., 2005. Continuous geomagnetic field models for the past 3 and 7 millenia : 1. A new global data compilation, *Geophys. Geochem. Geosyst.,* **6,** doi:10.1029/2004GC000800.

Lee, T.-Q., Lin, H.-S. & Liew, P.-M., 1998. Magnetic analysis on lacustrine deposits of Yuan-Yang Lake, northern Taiwan, *J. Geol. Soc. China,* **41,** 143–158.

Lu, R., Banerjee, S.K. & Marvin, J., 1990. Effects of clay mineralogy and the electrical conductivity of water on the acquisition of depositional remanent magnetization in sediments, *J. geophys. Res.,* **95,** 4531–4538.

Mingram, J., Allen, J.R.M., Brüchmann, C., Liu, J., Luo, X., Negendank, J.F.W., Nowaczyk, N. & Schettler, G., 2004. Maar– and crater lakes of the Long Gang Volcanic Field (N.E. China)—overview, laminated sediments, and vegetation history of the last 900 years, *Quat. Int.,* **123–125,** 135–147.

Ohno, M., Hamano, Y., Murayama, M., Matsumoto, E., Iwakura, H., Nakamura, T. & Taira, A., 1993. Paleomagnetic record over the past 35,000 years of a sediment core from off Shikoku, Southwest Japan, *Geophys. Res. Lett.,* **20,** 1395–1398.

Ohno, M., Hamano, Y., Okamura, M. & Shimazaki, K., 1991. Geomagnetic secular variation curve recorded in the sediments from Beppu Bay, Kyushu, Japan, *Rock Mag. Paleogeophys.,* **18,** 68–74.

Reimer, P.J. et al., 2004. IntCal04 Terrestrial Radiocarbon Age Calibration, 0—26 Cal Kyr BP, *Radiocarbon,* **46,** 1029–1058.

Rosenbaum, J., Reynolds, R., Smoot, J. & Meyer, R., 2000. Anisotropy of magnetic susceptibility as a tool for recognizing core deformation: reevaluation of the paleomagnetic record of Pleistocene sediments from drill hole OL-92, Owens Lake, California, *Earth planet. Sci. Lett.,* **178,** 415–424.

Tarling, D.H. & Hrouda, F., 1993. *The Magnetic Anisotropy of Rocks,* Chapman & Hall, London, 217 pp.

Usinger, H., 1991. Ein Stechbohrgerät zum Bergen von Torfen und Seesedimenten für Einsatz bis zu größeren Tiefen, in *Symposium on Palaeolimnology of Maar Lakes,* p. 55, eds Zolitschka, B. & Negendank, J.F.W., Bitburg, 1991.

Yamazaki, T., Joshima, M. & Saito, Y., 1983. Secular variation of a geomagnetic inclination since 9 000 yr B.P. in Japan recorded by sediments in Lake Kasumigaura, *Rock Magnetism Palaeogeophys.,* **10,** 23–28.

Yamazaki, T., Abdeldayem, A.L. & Ikehara, K., 2003. Rock-magnetic changes with reduction diagenesis in Japan Sea sediments and preservation of geomagnetic secular variation in inclination during the last 30,000 years, *Earth planet. Space,* **55,** 327–340.

Yancheva, G., 2003. Analyse der Remanenzträger und Rekonstruktion der geomagnetischen Paläosäkularvariationen Südostasiens – Magnetostratigraphische Bearbeitung von Sedimentkernen aus dem südostchinesischen Huguang Maar, *Dissertation thesis*, Universität Potsdam, Potsdam.

Yasuda, Y. & Catto, N., 2004. Environmental variability and human adaptation since the last glacial period: a volume dedicated to J.F.W. Negendank: A contribution of the Asian Lake Drilling Programme (ALDP), *Quat. Int.,* **123–125,** 1–6.

Zhu, R., Pan, Y. & Liu, Q., 1999. Geomagnetic excursions recorded in Chinese loess in the last 70 000 years, *Geophys. Res. Lett.,* **26,** 505–508.

Zhu, R.-X., Gu, Z.-Y., Huang, B.-C., Jin, Z.-X., Wei, X.-F. & LI, C.-J., 1994. Geomagnetic secular variations and climatic changes since 15 000 a B.P., Beijing Region, *Science in China,* **37,** 984–990.

Zhu, R.X., Coe, R.S. & Zhao, X.X., 1998. Sedimentary record of two geomagnetic excursions within the last 15 000 years in Beijing, China, *J. geophys. Res.,* **103,** 30 323–30 333.

Zhu, R., Guo, B., Pan, Y., Liu, Q., Zeman, A. & Zuchy, V., 2000. Reliability of geomagnetic secular variations recorded in a loess section at Lingtai, north-central China, *Science in China (Series D9,* **43,** 1–9.